THE ASTROPHYSICAL JOURNAL, 424:59–67, 1994 March 20

EINSTEIN X-RAY OBSERVATIONS OF THE CORE OF THE SHAPLEY SUPERCLUSTER IN NORTHERN CENTAURUS

JEFFREY BREEN, SOMAK RAYCHAUDHURY, WILLIAM FORMAN, AND CHRISTINE JONES
Harvard-Smithsonian Center for Astrophysics, 60 Garden Street, Cambridge, MA 02138
Received 1993 March 31; accepted 1993 September 24

ABSTRACT

We present *Einstein* X-ray observations of the core of the Shapley Supercluster, one of the richest and densest known mass concentrations in the local ($z < 0.1$) universe. We used Imaging Proportional Counter (IPC) observations supplemented with data from the *Einstein* Slew Survey to determine the locations and structure of mass concentrations in the region. An X-ray map composed of IPC observations of the central ($10° \times 10°$) region of the Shapley Supercluster is presented. We present evidence that the X-ray clusters observed within 5° of the core of the supercluster are on average brighter than those of corresponding richness class distributed throughout the sky. However, we measure no significant difference in the galaxy formation efficiency of these clusters of galaxies compared to other, more isolated clusters. We also find one previously uncataloged cluster-sized mass concentration in the core of the Shapley Supercluster. This new cluster, "SC 1327−312", is relatively X-ray bright ($F_x = 1.1 \pm 0.2 \times 10^{-11}$ erg s^{-1} cm^{-2} and $L_x = 1.1 \pm 0.2 \times 10^{44}$ ergs s^{-1} within 10′, assuming $z = 0.0477$, $H_0 = 50$, $q_0 = 0$). As SC 1327−312 lies well within an Abell radius of the richness $R = 4$ cluster Shapley 8 (A3558), we suggest it may contribute to an artificially high galaxy count and richness classification for Shapley 8. From slew data, we estimate an X-ray luminosity for Shapley 8 which is just half the mean luminosity of the four other $R = 4$ clusters observed by the IPC, further suggesting the richness classification to be an overestimate.

Subject headings: galaxies: clustering — X-rays: galaxies

1. INTRODUCTION

A great overdensity of galaxies in northern Centaurus was first noted by Shapley (1930). This region has received renewed attention as dynamical studies suggest the existence of a Hubble flow-perturbing "Great Attractor" in the Hydra-Centaurus direction (Lynden-Bell et al. 1988). Redshift studies of this region reveal two major mass concentrations: the nearer "Hydra-Centaurus Supercluster" at a mean redshift of 0.013 and the more distant "Shapley Supercluster" at a mean redshift of 0.046 (Melnick & Moles 1987; Raychaudhury 1989; Scaramella et al. 1989; Vettolani et al. 1990; Raychaudhury et al. 1991). The Hydra-Centaurus Supercluster is the closest known mass concentration to the predicted center of the Great Attractor, and, therefore, might be expected to contribute significantly to the peculiar velocity of the Local Group. The contribution from the Shapley Supercluster should not be as significant owing to its greater distance (Raychaudhury 1989), although recent work suggests that a more distant mass concentration might be responsible for bulk flows on still larger scales (Willick 1990; Mathewson, Ford, & Buchhorn 1992).

Aside from its potential cosmological importance, the Shapley Supercluster is of considerable interest due to its high galaxy density. Within just 5° of its optical core lie 2 rich clusters listed in the Abell Catalog, and 11 more in the southern supplement of non-Abell clusters (Abell 1958; Abell, Corwin, & Olowin 1989, hereafter ACO). Of the 19 clusters with known redshifts in this region, 16 appear to belong to the Shapley Supercluster: A3558 (Shapley 8; of Abell richness $R = 4$); A3559 and A3560 ($R = 3$); A3562, A3566, and A3571 ($R = 2$); and A3545, S726, A3555, S729, A3556, A3557, A1736, A3564, A3572, and A3575 ($R \leq 1$; redshifts from ACO and Vettolani et al. 1990). Vettolani et al. find that these clusters alone constitute an overdensity of at least a factor of 50 (90 if including only $R \geq 1$) compared to the expected distribution of Abell clusters at the same Galactic latitude ($|b| \approx 30°$). The Shapley Supercluster, thus, provides an extreme case where the effect of a dense supercluster environment on its member clusters can be studied. In this paper we use both X-ray and optical observations to compare the cluster richness/X-ray luminosity relation and the formation efficiency of galaxies for clusters in the Shapley Supercluster to that found for other present epoch clusters. We assume $H_0 = 50$ km s^{-1} Mpc^{-1} and $q_0 = 0$ throughout. Unless otherwise noted, all X-ray fluxes and luminosities are measured within the *Einstein* band of 0.5–4.5 keV.

2. OBSERVATIONS AND ANALYSIS

We have analyzed the *Einstein* imaging proportional counter (IPC) observations of the core of the Shapley Supercluster, from both pointed observations (Gorenstein, Harnden, & Fabricant 1981) and the Slew Survey (Elvis et al. 1992). We then compared this X-ray emission with the optical emission from the supercluster core from APM scans of IIIa-J plates obtained with the 1.2 m U.K. Schmidt Telescope (Raychaudhury 1990).

2.1. *Pointed X-Ray Observations*

There are 11 *Einstein* IPC pointed observations toward the Shapley Supercluster, and the majority of these are centered on X-ray clusters. While the full field of view of the IPC is $75' \times 75'$, the edges of the field are subject to increased background rates due to unrejected particle events, so the field of view is usually masked to a $60' \times 60'$ square. In order to increase sky coverage in the supercluster region, we used a special processing for each observation to obtain the full field, thus increasing coverage by 51%. To account for the background, we applied the same process to Deep Survey fields, which were then scaled by time and subtracted. We corrected each background-subtracted image for telescope vignetting

assuming a mean energy of 1.5 keV, typical of the peak of the observed energy distribution.

We co-added 11 such unmasked IPC observations to form a map of the central region of the Shapley Supercluster, within 5° of the map center, $\alpha(1950) = 13^h20^m$, $\delta(1950) = -30°$. Since each observation was taken for a different observation time, a corresponding "exposure map" proportional to the exposure time of each observation also was produced. These exposure maps contained corrections for the telescope vignetting as well as for the detector window support structure ("ribs"). Like the unmasked IPC fields, the exposure maps were similarly added into a mosaic and used to normalize the observations by time. Figure 1*a* shows the resulting X-ray map of the region, and Figure 1*b* contains an identification chart. The X-ray images reveal a region rich in substructure. The emission from A3528 clearly shows two components. There is strong evidence of substructure in A1736 from redshift studies (Dressler & Shectman 1988), and the X-ray emission from this cluster is fitted better by a two-component King profile than by a single-component model (Grant et al. 1994).

The pointed observation which is closest to the core of the Shapley Supercluster also reveals the most structure. IPC sequence I5730 is a 6.2 ks observation centered on $\alpha(1950) = 13^h29^m24^s$, $\delta(1950) = -31°26'$. Figure 2*a* shows the X-ray contours from this unmasked observation overlaid upon the SRC IIIa-J plate of the region, while Figure 2*b* provides an identification chart for the observation. The field is nominally centered on the poor cluster SC 1329−313, but also contains A3562 to the east. A previously uncataloged cluster-sized mass concentration is apparent at the extreme western edge of the field. Only four galaxies have measured redshifts within 10′ of the center of this new concentration—and none of these lie within 5′ of the X-ray center (see Table 1). As all four redshifts are consistent with that of Shapley 8, this concentration is probably a new cluster closely associated with Shapley 8, or perhaps a major subcluster of Shapley 8 itself. We denote this concentration "SC 1327−312" and assign to it the redshift of Shapley 8 ($z = 0.0477$; Teague, Carter, & Gray 1990). Together, Shapley 8, SC 1327−312, SC 1329−313, and A3562 form a remarkable linear structure on the sky, lying along an almost straight line ~1° long (~4.5 Mpc) with rich Abell clusters at each end.

In order to derive physical parameters for each cluster apparent in Figure 1*a*, observations were compared to a simple empirical model for the X-ray surface brightness distribution. A radial surface brightness profile of each cluster was obtained,

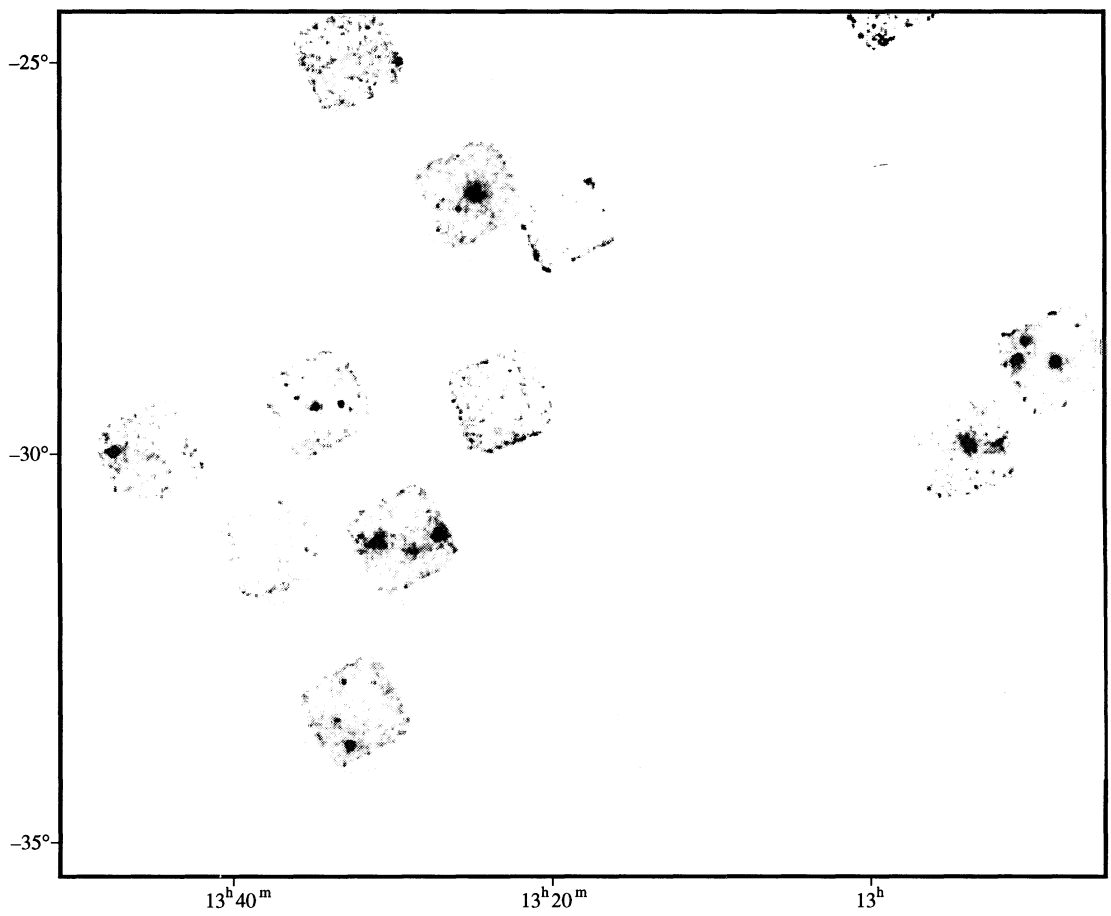

FIG. 1*a*

FIG. 1.—(*a*) Thirteen unmasked *Einstein* IPC observations have been co-added to form this map of the Shapley Supercluster in the Hydra-Centaurus region. The X-ray emission has been added into 1′ × 1′ bins, and smoothed with a Gaussian of $\sigma = 1'$. (*b*) Identification chart for (*a*). The outline of the IPC detector is shown for each pointed observation. Filled circles denote emission from clusters of galaxies believed to be a part of the Shapley Supercluster. Open circles denote other X-ray clusters. The filled diamond denotes emission detected from Shapley 8 in the Slew Survey. Open squares denote all other identified sources.

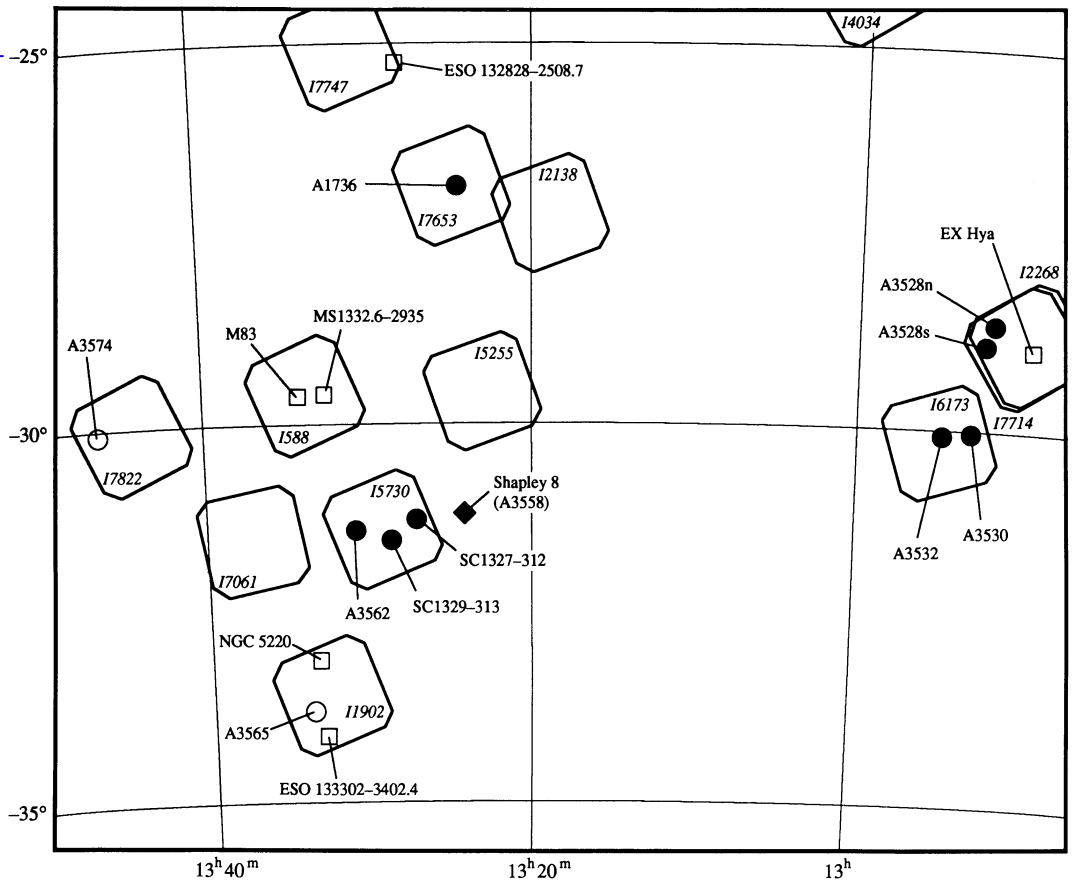

FIG. 1*b*

TABLE 1

REDSHIFTS FOR SC 1327−312 AND SC 1329−313

CLUSTER NAME	z	GALAXY POSITION (1950) R.A.	Decl.	$V_\odot$	SOURCE
SC 1327−312.....	0.0477[a]	13h26m21s.0	−31°17′20″	14674	T
		13 26 21.1	−31 18 19	12282	T
		13 26 31.7	−31 16 57	13262	R
		13 26 39.0	−31 17 30	15419	FC
SC 1329−313.....	0.0438	13 28 26.9	−31 31 10	13359	Q
		13 28 36.0	−31 36 00	13007	SG
		13 28 38.1	−31 33 43	12921	Q
		13 28 43.9	−31 33 20	13102	Q
		13 29 12.0	−31 39 48	(4505)[b]	dC
		13 29 01.2	−31 33 15	13336	Q
		13 29 13.4	−31 31 22	13107	FC

NOTES.—Redshifts for galaxies within the diffuse X-ray emission of the clusters SC 1327−312 and SC 1329−313. There is no measured redshift within 5′ of the core of SC 1327−312, however, so the redshift of Shapley 8 from Vettolani et al. 1990 is assumed. One of the galaxies with measured redshifts in SC 1329−313 appears to be a member of the nearer Hydra-Centaurus Supercluster and is excluded from the redshift calculation. Redshift sources: Q, Quintana et al. 1994; T, Teague, Carter, & Gray 1990; R, Richter 1987; dC, da Costa et al. 1987; FC, SG, Fairall Catalog, Schombert & Gregg (private communication), both as cited in the redshift compilation of J. Huchra.

[a] Computed redshift is 0.0464, but no galaxy with a measured redshift lies within 5′ of the central galaxy, so the redshift of Shapley 8 ($z = 0.0477$) from Teague et al. 1990 is assumed.

[b] This galaxy's redshift is consistent with the foreground Hydra-Centaurus Supercluster. It has been excluded from the redshift calculation.

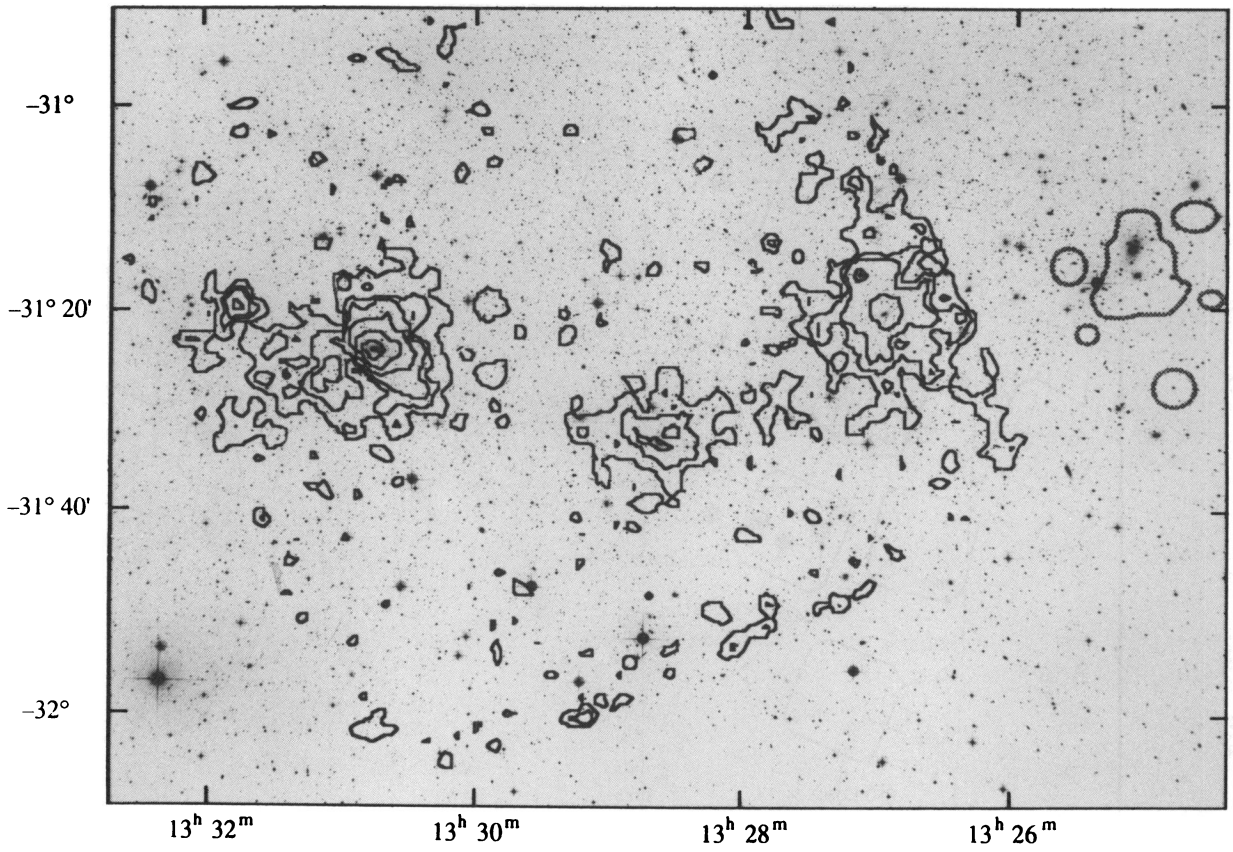

FIG. 2a

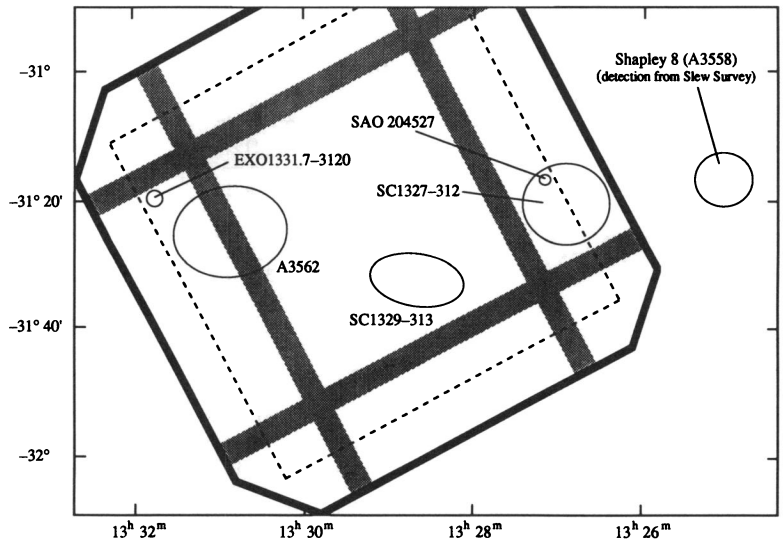

FIG. 2b

FIG. 2.—(*a*) X-ray contours from the unmasked IPC observation I5730 overlaid upon SRC plate 444 of the region. The image was smoothed with a Gaussian of $\sigma = 32''$ and contours were drawn at 5%, 10%, 15%, 30%, 50%, and 80% of the peak. The grey markings to the west of the figure represent emission from Shapley 8 detected as the instrument slewed through the region. (*b*) An identification chart for Fig. 2*a*. The full IPC field is shown as a rotated 75′ square with truncated corners. The dashed square indicates the 60′ × 60′ field of view normally preserved by the Standard Processing. The large cross-hatched pattern represents the shadow cast upon the detector by the IPC detector window support structure "ribs." The following sources are identified and labeled: SC 1327−312, SAO 204527, SC 1329−313, A3562, and EXO 1331.7−3120. SAO 204527 is a K2 star whose X-ray emission contaminates the northeast corner of SC 1327−312. (*c*) The optical emission from the same region. Galaxy emission has been corrected for internal and Galactic extinction, collected into 1′ × 1′ bins, and smoothed with a Gaussian of $\sigma = 1'.5$. The contours correspond to 0.25, 0.5, 0.75, 1.0, 1.5, and 2.0 in units of L^*, assuming a universal M_j^* of −19.4 at the redshift distance of Shapley 8 (286 Mpc).

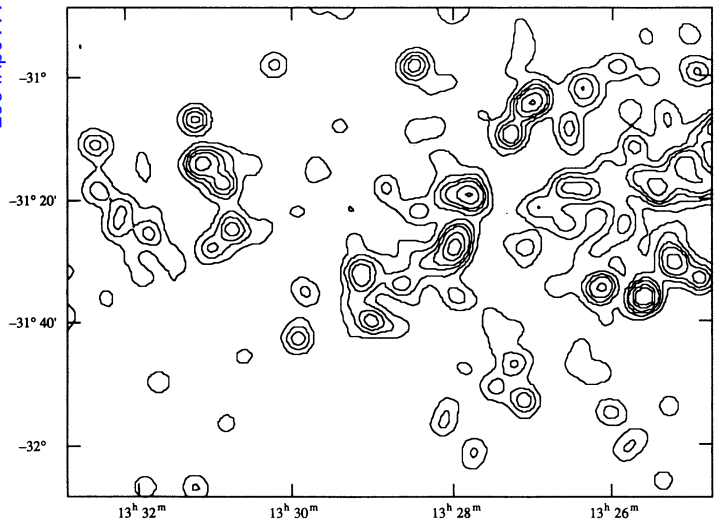

FIG. 2c

assuming azimuthal symmetry about the X-ray center. A simple model of the surface brightness given by

$$S(r) = S_0\left[1 + \left(\frac{r}{a}\right)^2\right]^{-3\beta+1/2}, \quad (1)$$

where a is a characteristic radius and β is a free parameter, is convolved with the instrument's point response function before comparison with the data (as described in Jones & Forman 1984). Due to the geometry of some of the observations, extreme care was necessary in extracting radial profiles. A3562 is nearly bisected by the shadow from a detector window support structure "rib," SC 1329−313 lies close to another, and SC 1327−312 is observed entirely in the narrow region between the "rib" and the edge of the detector (see Fig. 2*b*). It was therefore impossible to extract source counts beyond 15′ from the centers of SC 1327−312 and SC 1329−313. For A3562, it was necessary to extract source counts from a pie-wedge region normal to the rib, and extrapolate accordingly.

Since the X-ray emissivity of gas within the 0.5–4.5 keV *Einstein* band is rather insensitive to temperature changes within the 2–10 keV range, the surface brightness profile determined with the IPC is a good measurement of the emission integral of the emitting gas (Canizares et al. 1982; Abramopoulos & Ku 1983). The X-ray luminosity observed within a radius R is due to the gas within a cylindrical volume along the line of sight to the cluster, and is given by

$$L_x(R) = \frac{2\pi n_e n_p \Lambda a^3}{(1-3\beta)} \times \int_0^\infty \left\{\left[1 + s^2 + \left(\frac{R}{a}\right)^2\right]^{1-3\beta} - (1+s^2)^{1-3\beta}\right\} ds, \quad (2)$$

where a and β are defined as before, n_e is the central electron number density, n_p is the central number density of hydrogen nuclei, Λ is the radiative cooling coefficient of the emitting gas, and s is the distance through the cluster in units of the characteristic radius, a. The radiative cooling coefficient, A, depends on the gas temperature, while a and β are measured from the surface brightness distributions. The central densities $n_e n_p$ can be determined by comparing the model of the emission (2) with the observed flux within a radius R. We estimate the mass of the X-ray emitting gas from the surface brightness profile, assuming spherical symmetry. Table 2 summarizes observed and calculated parameters for the clusters observed in the central region of the supercluster.

2.2. *Einstein Slew Survey Data*

The gray markings near the western edge of Figure 2*a* are not contours from a pointed observation, but denote emission from Shapley 8 detected while the satellite was slewing. Although the *Einstein* mission was primarily a pointed one, the recent Slew Survey contains data recorded as the telescope slewed from one pointed observation to another (Elvis et al. 1992; Plummer et al. 1991). As there were several IPC targets in this area of the sky, slew survey coverage of the region is fairly complete spatially, though the average exposure time near Shapley 8 is only 10 s. Even with such limited exposure time, the slew data can be used to determine the position of the X-ray emission associated with Shapley 8, and to estimate its flux and luminosity. The Slew Survey catalog includes both of the Abell clusters in the region: Shapley 8 (1ES 1325−312) and A3562 (1ES 1330−313). The poor cluster SC 1329−313 is evident in the data, although too weak to be detected as a source in the catalog. The cluster SC 1327−312 is listed as 1ES 1327−313, although both it and Shapley 8 are misidentified as SAO stars due to the survey's procedure to find optical counterparts (Schachter et al. 1994).

An overall normalization constant to account for background and other corrections was derived by comparing the slew and pointed detections of the cluster SC 1327−312, the brightest cluster to appear in its entirety in both observations. Shapley 8 is the brightest X-ray source near the core, with an estimated counting rate of 1.4 ± 0.4 counts s^{-1} within a 10′ radius from its optical center. This counting rate, combined with a gas temperature of 6.2 keV determined by *GINGA* (Day et al. 1991), implies a 0.5–4.5 keV X-ray luminosity of $5.4 \pm 1.4 \times 10^{44}$ ergs s^{-1}. As the slew data are so sparse, we cannot determine the morphology of the emitting region, leaving open the question of additional substructure within Shapley 8 itself. Perhaps more important than allowing an estimate of the luminosity of Shapley 8, the slew data confirm that the cluster SC 1327−312 identified in the pointed observation is a second mass concentration and not the main center of X-ray emission associated with Shapley 8.

2.3. *Optical Luminosities*

To compare the X-ray emission to the optical emission from these clusters, we used IIIa-J plates from the 1.2 m U.K. Schmidt Telescope in Australia. The Automated Photographic Measuring (APM) facility in Cambridge (England) was used to find images on these plates, and an automated algorithm (Raychaudhury 1990) was used to isolate nonstellar images from this list using the profile and intensity parameters measured by the APM. All of these images were inspected by eye, galaxies were identified, and morphological types assigned to them. The APM measures accurate positions and B_J magnitudes for these galaxies, the latter being calibrated by CCD photometry (Raychaudhury et al. 1994).

As previous studies have already investigated other clusters distributed throughout the supercluster (Raychaudhury 1990; Raychaudhury et al. 1991), we concentrate our optical study on the three clusters in the central *Einstein* pointed observation in which SC 1327−312 was discovered. We chose all galaxies in the APM catalog brighter than $B_J = 18.2$ that lie in this

TABLE 2

X-RAY CLUSTERS SHOWN IN MAP OF SHAPLEY SUPERCLUSTER

CLUSTER NAME	X-RAY EMISSION CENTER (1950)		ABELL CATALOG		CLUSTER REDSHIFTS		*Einstein* IPC SEQUENCE NUMBER	L_x TO 1 Mpc (10^{44} ergs s^{-1})	KING MODEL PARAMETERS		CENTRAL n_p (10^{-3} cm^{-3})	GAS MASS TO 1 Mpc (10^{13} $M_\odot$)	OTHER NAMES
	R.A.	Decl.	Richness Class	Galaxy Count	z	Number			a (Mpc)	β			
A3528n	$12^h51^m38^s.2$	$-28°44'01''$	1	70	0.0535	39	2268, 7714	1.4 ± 0.2	0.25	0.60	1.6 ± 0.1	3.4 ± 0.4	K21
A3528s	12 51 58.5	−28 57 20						1.7 ± 0.3	0.25	0.60	1.7 ± 0.2	3.6 ± 0.5	...
A3530	12 52 51.7	−30 03 54	0	34	0.0544	5	6173	0.8 ± 0.1	0.25	0.60	1.2 ± 0.1	2.6 ± 0.3	...
A3532	12 54 38.9	−30 06 13	0	36	0.0539	44	6173	2.7 ± 0.4	0.35 ± 0.13	0.61 ± 0.10	1.5 ± 0.3	4.9 ± 1.6	K22
A1736	13 24 12.7	−26 54 40	0	41	0.0461	63	7653	1.4 ± 0.2	0.40 ± 0.13	0.73 ± 0.22	1.1 ± 0.1	3.4 ± 0.4	IC 4255
Shapley 8	13 25 06.0	−31 14 00	4	226	0.0477	≥100	Slew	5.4 ± 1.4	...	...	...	...	A3558
SC 1327−312	13 26 56.3	−31 20 43			0.0477[a]	0	5730	1.3 ± 0.3	0.33 ± 0.01	0.60	1.1 ± 0.1	3.4 ± 0.5	...
SC 1329−313	13 28 46.4	−31 33 19	2	129	0.0438[b]	6	5730	0.5 ± 0.1	0.34 ± 0.01	0.60	0.7 ± 0.1	2.2 ± 0.3	...
A3562	13 30 42.1	−31 24 14			0.0502	12	5730	2.7 ± 0.4	0.20 ± 0.01	0.60	3.0 ± 0.3	4.6 ± 0.6	...

NOTES.—X-ray positions and parameters for the nine clusters of galaxies visible in Fig. 1*a*. Redshifts are from the compilation of Vettolani et al. 1990, except as noted. A calibration uncertainty of 15% has been assumed for the luminosities except for Shapley 8 and SC 1327−312 where 25% is more appropriate. King model parameter uncertainties correspond to the 90% confidence level, while those without errors listed are default values and were not fitted explicitly (Jones & Forman 1993).

[a] Lacking redshift measurements, we assume the same redshift as for Shapley 8.

[b] Redshift computed in this paper (see text and Table 1).

region. We corrected each galaxy magnitude for internal extinction, as prescribed by the RC3 catalog (de Vaucouleurs et al. 1991), and applied a uniform correction for Galactic absorption of $0^m.3$ (the mean extinction in B for the core region of the Shapley Supercluster from Burstein & Heiles 1982). Background galaxies were accounted for with the magnitude distribution function inferred from the APM South Galactic Pole bright galaxy survey, which is the source of the Stromlo–APM Redshift Survey (Loveday et al. 1992). Figure 2*c* shows the distribution of optical galaxy emission in this region, where the light in each $1' \times 1'$ bin has been smoothed with a Gaussian of $\sigma = 1'.5$. The contours are drawn at 0.25, 0.5, 0.75, 1.0, 1.5, and 2.0 in units of L^*, assuming a universal M_J^* of -19.4 (Efstathiou, Ellis, & Peterson 1988) and the redshift distance of Shapley 8 (286 Mpc).

We used the B_J magnitudes in the APM catalog to derive the optical luminosities for the three clusters evident in the central *Einstein* pointed observation, using their redshifts (as listed in Table 2) to infer their distance. The luminosity distribution within 1 Mpc of the X-ray center of each cluster was fitted to the cumulative form of a Schechter luminosity function,

$$\Phi(>L) = N_0 Q_0\left(1+\alpha, \frac{L}{L_*}\right), \quad (3)$$

where $Q_0(a, t)$ is the Incomplete Gamma Function. In order to reduce the parameters of the fit, we fixed the value of the "slope" α to be equal to -1, and treated N_0 and L^* as free parameters. This value for the slope is consistent with the results of Efstathiou et al. (1988) and reduces the solution to an exponential integral. A 20% change in the slope used to fit the luminosity functions changes the resulting total luminosities by less than 3%. Correcting for the light due to galaxies fainter than our magnitude limit, we find B_J luminosities within 1 Mpc of the cluster centers of $1.7 \times 10^{12}\ L_\odot$ for SC 1327−312, $1.8 \times 10^{12}\ L_\odot$ for SC 1329−313, and $1.5 \times 10^{12}\ L_\odot$ for A3562. Note that these values are not correlated with the "Abell richness" for these clusters (indeed, the first two are not classified as rich clusters in the ACO catalog), since these richness estimates are not meaningful when there is considerable overlap between the Abell radii of neighboring clusters as is often true in supercluster cores. Much of the uncertainty in these luminosities is due to the small number of galaxies within 1 Mpc with which to determine a magnitude distribution. Deeper APM scans or CCD observations should allow for better accuracy in the future. Subtracting background galaxies in such a dense region is difficult, and is further complicated for SC 1327−312 by the proximity of Shapley 8.

3. DISCUSSION

The X-ray images of the core of the Shapley Supercluster show much substructure, also reflected in galaxy count distributions (Raychaudhury et al. 1991). As expected, Shapley 8 (A3558), the richest Abell cluster near the core of the Shapley Supercluster, is also the most X-ray luminous, but it is not as bright as expected for its richness, as found from *GINGA* observations by Day et al. (1991). They report the X-ray luminosity of Shapley 8 measured in the *GINGA* 2–10 keV band to be only 30% that of A1689, another richness 4 cluster. Similarly, our estimated *Einstein* 0.5–4.5 keV luminosity for Shapley 8 is only 23% of that measured for A1689 (Jones & Forman 1993). Furthermore, Shapley 8's luminosity is only 45% that of the mean of the four other richness 4 clusters measured by the *Einstein* IPC (see Table 3).

Burg et al. (1993) present X-ray luminosity functions for clusters of richness classes $R = 0$–2. A3562 falls below the 25th percentile of 6.0×10^{43} ergs s^{-1} for $R = 2$ clusters. However, the richness classification of A3562 is almost certainly an overestimate as SC 1329−313 and part of SC 1327−312 fall within one Abell radius of its optical center. The X-ray emission from A3562 is more characteristic of a $R = 1$ or a bright $R = 0$ cluster. The underluminosity of both Shapley 8 and A3562 is easily explained as an overestimation of cluster richness due to optical contamination in a crowded region. The X-ray luminosity within a given radius (such as 1 Mpc) may be a more useful indication of cluster richness than optical galaxy counts in dense regions such as supercluster cores.

But while the rich clusters Shapley 8 and A3562 appear fainter than their Abell richness classifications, would predict, the poorer clusters observed within 5° of the supercluster core are actually brighter than expected. Each of the three $R = 0$ clusters in our sample is above the median luminosity of 3.5×10^{43} ergs s^{-1}, and two of these (A3532 and A1736) are above the 75th percentile of 10^{44} ergs s^{-1}. Each component of A3528 alone is almost as bright as the 75th percentile for $R = 1$ clusters, the richness class assigned to both components *together*.

If we make several assumptions about cluster evolution, it is possible to estimate the galaxy formation efficiency of a cluster given its X-ray gas and optical stellar masses. We assume that clusters are closed systems: galaxies form from the intracluster medium (ICM); the mass ejected from the galaxies during their evolution is small compared to the amount of gas left over from their formation; and no ICM is lost from the cluster over time. In this scenario, the formation efficiency of the galaxies in clusters may be simply expressed as

$$\epsilon = \left(1 + \frac{M_{\rm gas}}{M_{\rm stellar}}\right)^{-1}, \quad (4)$$

where $M_{\rm gas}$ and $M_{\rm stellar}$ represent the baryonic cluster mass in gas and stars, respectively. This relation also assumes that the dark matter is not baryonic. Using a sample of several clusters ranging from poor groups to rich clusters, David et al. (1990) showed a strong relation between galaxy formation efficiency and the depth of the cluster potential well, as characterized by the temperature of the ICM. To make our sample consistent with that of David et al., we fitted King density profiles to the galaxy data for each of our clusters and extrapolated the optical luminosity to five core radii. We then computed the

TABLE 3

X-RAY PROPERTIES OF ABELL RICHNESS 4 AND 5 CLUSTERS OBSERVED BY THE EINSTEIN IPC

Cluster Name	L_x (10^{44} ergs^{-1})	Notes
A545	10.8 ± 1.1	...
A665	12.2 ± 1.2	$R = 5$
A1146	3.4 ± 0.3	...
A1689	22.8 ± 2.3	...
Shapley 8	5.4 ± 1.4	Estimated from the Slew Survey
A2218	9.3 ± 0.9	...

NOTES.—X-ray parameters for those Abell richness 4 and 5 clusters observed by the *Einstein* IPC from Jones & Forman (1993). Both A1146 and Shapley 8 are conspicuous in their low luminosities.

galaxy's luminosities neglecting internal extinction, and converted these luminosities to the V-band using the morphological information from our optical catalog. We chose $M_{gas}/L_{stellar}$ as an indicator of galaxy formation efficiency rather than assuming a mass to light ratio to infer $M_{stellar}$ as in equation (4).

Figure 3*a* shows our sample of three clusters from the core of the Shapley Supercluster merged with the larger sample of David et al. (1990). Cluster gas temperatures not measured are estimated from the temperature-luminosity relationship determined from *Einstein*, *EXOSAT*, and *Ginga* results (David et al. 1993). The three core clusters follow the same trend as the earlier sample, within the scatter of the established relationship, suggesting that the galaxy formation efficiency in clusters is fairly independent of the local supercluster environment. A1631 is the only other member of the Shapley Supercluster for which suitable data exist for inclusion in this comparison. It does not fit the established relation well, but it should be noted that due to its unusually large X-ray core radius ($a = 0.71$ Mpc), it has only been extrapolated to 1 Mpc. Since the gas temperatures for these clusters are only estimates, we also compare the mass in the ICM with the measured optical luminosity from their galaxies. Figure 3*b* shows that the clusters in the Shapley Supercluster obey the same relationship between the mass of the X-ray emitting gas (M_x) and the total visual luminosity of the galaxies (L_v), best characterized by

$$M_x \propto L_v^{1.32 \pm 0.29} (1\ \sigma \text{ error}) \quad (5)$$

in agreement with previous results for more isolated clusters (e.g., Arnaud et al. 1992).

While larger samples of clusters with observed X-ray and optical properties are available, they usually include data from many different observers and instruments and inevitably suffer from inconsistent or inappropriate methodologies. The sample of Arnaud et al. (1992), for example, contains more than two dozen clusters drawn from more than a half dozen sources. Moreover, these cluster luminosities and masses are extrapolated to 3 Mpc, which is inappropriate for dense, crowded regions, such as the core of a supercluster. Accordingly, we are presently engaged in an effort to compile a larger, consistent sample using *Einstein* and *ROSAT* X-ray observations and deep CCD exposures.

In summary, we find that the properties of clusters in the core of the Shapley Supercluster, as measured through their X-ray emission and compared with their optical emission, are quite similar to those found for more isolated systems. In particular, their core radii are typical of other rich clusters, and their gas masses are comparable to other systems. Like nearly half of all clusters, these clusters show considerable substructure. While the poorer clusters within 5° of the supercluster center are on average brighter than clusters of the same richness, the richer clusters in this region are fainter than expected, since the relatively large radius chosen by Abell (3 Mpc) leads to significant overestimates of richness in regions of high galaxy density and substructure such as this supercluster. Finally, these supercluster members show the same relationship between the mass in the galaxies and the mass of the ICM as do more isolated clusters. These findings lead us to conclude that the formation processes for galaxies and clusters are relatively independent of the environment outside the clusters, even when that environment is a dense supercluster core.

The authors wish to thank Carolyn Stern and Tony Loesser for their assistance in processing the IPC data and John Roll for the code to co-add the pointed observations. Cathy Clemens was very helpful in providing redshifts for this region. This research has made use of the NASA/IPAC Extragalactic Database (NED) which is operated by the Jet Propulsion Laboratory, California Institute of Technology, under contract with the National Aeronautics and Space Administration. This work has been supported by NASA Grant NAG 5-1204. S. R. is supported by a Smithsonian postdoctoral fellowship at the CfA.

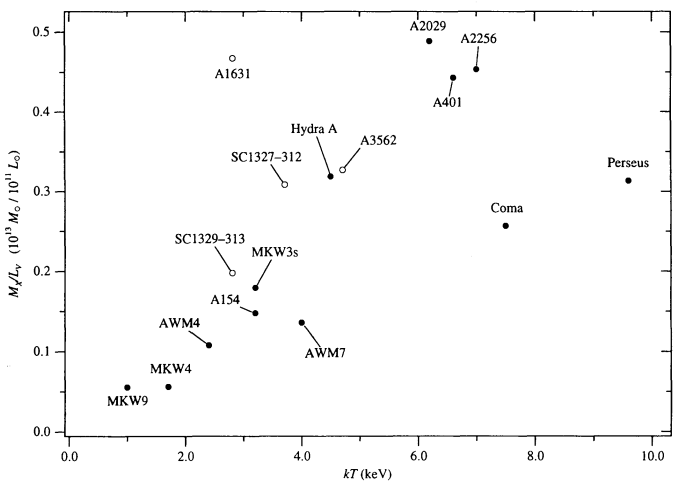

FIG. 3*a*

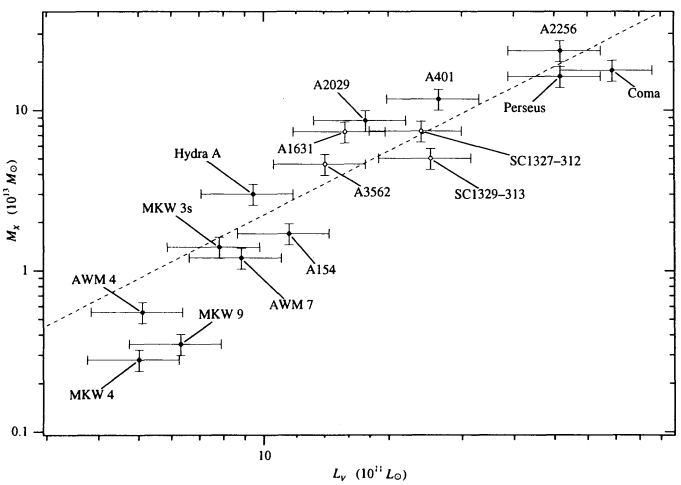

FIG. 3*b*

FIG. 3.—(*a*) The ratio of X-ray gas mass to optical luminosity within five X-ray core radii is plotted as a function of the gas temperature of the intracluster medium for the clusters in the Shapley Supercluster (*open circles*) and for the sample of poor groups to rich Abell clusters (*filled circles*) of David et al. (1990). (A1631 has only been extrapolated to 1 Mpc due to its large X-ray core radius.) If the mass follows the light, the ratio of gas mass to optical luminosity is directly proportional to the ratio of gas mass to optical mass, and can be interpreted as being inversely proportional to the galaxy formation efficiency of the cluster (see text). Note that the three clusters from the core of the Shapley Supercluster, a very dense supercluster region, do not significantly deviate from the relation for more isolated clusters. (*b*) The three core clusters (*open circles*) also follow the same relationship between X-ray gas mass and total visual luminosity as do the clusters from the sample of David et al. (*filled circles*). Uncertainties for the gas masses are computed for our sample (see Table 1) and assumed to be 15% for the larger sample. Twenty-five percent uncertainties are shown for the visual luminosities.

REFERENCES

Abell, G. 1958, ApJS, 3, 211
Abell, G., Corwin, H. G., & Olowin, R. 1989, ApJS, 70, 1
Abramopoulos, F., & Ku, W. H. 1983, ApJ, 271, 446
Arnaud, M., Rothenflug, R., Boulade, O., Vigroux, L., & Vangioni-Flam, E. 1992, A&A, 254, 49
Burg, R., Giacconi, R., Forman, W., & Jones, C. 1994, ApJ, 422, 37
Burstein, D., & Heiles, C. 1982, AJ, 87, 1165
Canizares, C., Clark, G., Jernigan, J., & Markert, T. 1982, ApJ, 262, 33
da Costa, L. N., Willmer, C., Pellegrini, P. S., & Chincarini, G. 1987, AJ, 93, 1338
David, L. P., Arnaud, K. A., Forman, W., & Jones, C. 1990, ApJ, 356, 32
David, L. P., Slyz, A., Jones, C., Forman, W., Vrtilek, S. D., & Arnaud, K. A. 1993, ApJ, 412, 479
Day, C. S. R., Fabian, A. C., Edge, A. C., & Raychaudhury, S. 1991, MNRAS, 252, 394
de Vaucouleurs, G., de Vaucouleurs, A., Corwin, H., Buta, R., Paturel, G., & Fouqué, P. 1991, Third Reference Catalogue of Bright Galaxies (New York: Springer)
Dressler, A., & Shechtman, S. A. 1988, AJ, 95, 284
Efstathiou, G., Ellis, R. S., & Peterson, B. A. 1988, MNRAS, 232, 431
Elvis, M., Plummer, D., Schachter, J., & Fabbiano, G. 1992, ApJS, 80, 257
Gorenstein, P., Harnden, R. F., & Fabricant, D. G. 1981, IEEE Trans. Nucl. Sci., NS-28, 869
Grant, C., Hughes, J., Jones, C., & Forman, W. 1994, in preparation
Jones, C., & Forman, W. 1984, ApJ, 276, 38
———. 1993, private communication
Loveday, J., Peterson, B. A., Efstathiou, G., & Maddox, S. J. 1992, ApJ, 390, 338
Lynden-Bell, D., Faber, S. M., Burstein, D., Davies, R. L. Dressler, A., Terlevich, R. J., & Wegner, G. 1988, ApJ, 326, 19
Mathewson, D. S., Ford, V. L., & Buchhorn, M. 1992, ApJ, 389, L5
Melnick, J., & Moles, M. 1987, Rev. Mex. Astron. Af., 14, 72
Plummer, D., Schachter, J., Garcia, M., & Elvis, M. 1991, The *Einstein Obs.* SLEW Survey (Version 1.0, 1991, Jan. 1), CD-ROM issued by Smithsonian Astrophysical Ob.
Quintana, H., Ramirez, A., Raychaudhury, S., Melnick, J., & Slezak, E. 1994, in preparation
Raychaudhury, S. 1989, Nature, 342, 251
———. 1990, Ph.D. thesis, Univ. Cambridge, England
Raychaudhury, S., Fabian, A. C., Edge, A. C., Jones, C., & Forman, W. 1991, MNRAS, 248, 101
Raychaudhury, S., Scharf, C., Williger, G., & Lynden-Bell, D. 1994, in preparation
Richter, O.-G. 1987, A&AS, 67, 261
Scaramella, R., Baiesi-Pillastrini, G., Chincarini, G., Vettolani, G., & Zamorani, G. 1989, Nature, 338, 562
Schachter, J., et al. 1994, in preparation
Shapley, H. 1930, Bull. Harvard Obs., 874, 9
Teague, P. F., Carter, D., & Gray, P. M. 1990, ApJS, 72, 715
Vettolani, G., Chincarini, G., Scaramella, R., & Zamorani, G. 1990, AJ, 99, 6
Willick, J. A. 1990, ApJ, 351, L5